

## Finite Element Simulation of Angular Distortion In Carbon Steel Butt Welded Joint

Hitesh Arora<sup>1</sup>, Prashant K. Pandey<sup>2</sup>, Mandeep Singh<sup>3</sup>, Vishaldeep Singh<sup>4</sup>

<sup>1234</sup>Assistant Professor, Lovely Professional University

<sup>1</sup>[hitesh.15774@lpu.co.in](mailto:hitesh.15774@lpu.co.in), <sup>2</sup>[prashant.15821@lpu.co.in](mailto:prashant.15821@lpu.co.in) <sup>3</sup>[mandeep.15984@lpu.co.in](mailto:mandeep.15984@lpu.co.in),

<sup>4</sup>[vishaldeep.15837@lpu.co.in](mailto:vishaldeep.15837@lpu.co.in)

### Abstract

A computational procedure is presented for analyzing the angular distortion in carbon steel butt-welded joint. Based on the ANSYS software, uncoupled thermal-mechanical three-dimensional (3-D) finite element model was developed. The distortion of welded plate is found to be a nonlinear problem in geometry and material; therefore, the finite element solution is based upon the thermo-elasto-plastic and large deflection theory. The complex phenomenon of submerged arc welding is numerically solved by sequentially coupled transient, non-linear thermo-mechanical analysis. In this paper we studied the effects of welding and design parameters like welding current, welding speed and thickness of the plate. The simulated result shows that the angular distortion increases with the increase in heat input per unit area.

**Keywords:** FEM, Submerged Arc Welding, Distortion, Temperature Variation

### Introduction

Metallic structures in industry are assembled through some kind of welding process which is composed of heating, melting and solidification using a heat source such as arc, laser, torch or electron beam. The highly localized transient heat and strongly nonlinear temperature fields in both heating and cooling processes cause non-uniform thermal expansion and contraction, and thus result in plastic deformation in the weld and surrounding areas [1].

In fusion welding, a source of energy is necessary to cause the required melting of the materials to be joined. Even after the net energy from the source is transferred to the work-piece as heat, not all of that heat contributes to cause melting to produce the weld. Some is conducted away from the point of deposition, raising the temperature of material surrounding the zone of fusion and causing unwanted metallurgical and geometric changes [2].

Distortion occurs as a result of unbalanced thermally induced stresses, if the material or structure is free to respond to those unbalanced stresses, that is, if the material or structure is not restrained. Residual stresses occur as the result of unbalanced thermally induced stresses, being prevented from causing distortion, and, thereby, being partially relieved, when the material or structure is restrained. Thus, it should come as no surprise that attempting to prevent or reduce distortion must be done in such a way that intolerable residual stresses do

not result instead. Contrarily, attempting to relieve residual stresses once they have developed from welding must be done in such a way that unacceptable distortion does not result [3].

### A. Generalized Equation of Heat Flow

The thermal conditions in and near the fusion zone of a fusion weld must be maintained within specific limits to control metallurgical structure, residual stresses and distortions, and chemical reactions (e.g. oxidation) that result from a welding operation.

The transfer of heat in a weldment is governed primarily by the time- dependent conduction of heat, which is expressed by the following general equation of heat flow [Bergheau 2008]:

$$\rho c \frac{dT}{dt} = \frac{dq_x}{dx} + \frac{dq_y}{dy} + \frac{dq_z}{dz} - \rho c \left( V_x \frac{dT}{dx} + V_y \frac{dT}{dy} + V_z \frac{dT}{dz} \right) + Q \quad \dots (1)$$

Here  $q_x$ ,  $q_y$  and  $q_z$  are components of heat flow through the unit area;  $Q = Q(x; y; z; t)$  is the inner heat generation rate per unit volume;  $\rho$  is material density;  $c$  is heat capacity;  $T$  is temperature and  $t$  is time. According to the Fourier's law the components of heat flow can be expressed as follows

$$q_i = k \frac{dT}{di} \quad \dots (2)$$

where  $k$  is the thermal conductivity coefficient of the isotropic media and  $i = x, y$  and  $z$ . Substitution of Fourier's relations (2) in equation (1) gives the following basic heat transfer equation

$$\rho c \frac{dT}{dt} = \frac{d}{dx} \left[ k \frac{dT}{dx} \right] + \frac{d}{dy} \left[ k \frac{dT}{dy} \right] + \frac{d}{dz} \left[ k \frac{dT}{dz} \right] - \rho c \left( V_x \frac{dT}{dx} + V_y \frac{dT}{dy} + V_z \frac{dT}{dz} \right) + Q \dots (3)$$

For the transient thermal analysis thermal conductivity and specific heat are assumed to depend on temperature. Density is assumed to be constant. Heat generation is assumed to follow the Double Ellipsoidal heat distribution [5] and modelled as moving heat source in the present work.

## Modeling Methodology

### A. Heat Source Model

Goldak and Akhlaghi [4] observed that the temperature gradient in front of the heat source was not as steep as expected and the temperature gradient at the trailing edge of the molten pool was steeper than experimental measurements. To overcome this limitation Goldak and Akhlaghi [4] proposed a Double Ellipsoidal heat sources combining the front and rear half of the ellipsoidal power density heat distribution of equation (4 & 5). The schematic of the Double Ellipsoidal heat distribution is depicted in Figure 1. The Double Ellipsoidal heat distribution of the power density in coordinate axes ( $x, y, z$ ) is given by

$$q_f(x, y, z, t) = \frac{6\sqrt{3}f_f Q}{abc\pi\sqrt{\pi}} e^{-3x^2/a^2} e^{-3y^2/b^2} e^{-3[z+v(\tau-t)]^2/c^2} \dots (4)$$

and for the rear half

$$q_r(x, y, z, t) = \frac{6\sqrt{3}f_r Q}{abc\pi\sqrt{\pi}} e^{-3x^2/a^2} e^{-3y^2/b^2} e^{-3[z+v(\tau-t)]^2/c^2} \dots (5)$$

where  $f_f$  and  $f_r$  are the fractions of heat deposited in the front and rear quadrants with  $f_f + f_r = 2$ . The parameters  $a$ ,  $b$ ,  $c$  define the ellipsoidal distribution and can have different values in the front and rear quadrants since front and rear half are independent.

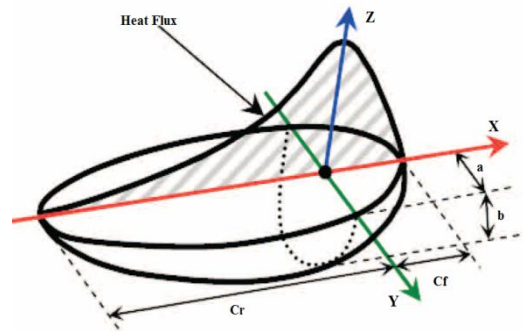


**Figure 1:** Configuration of Double Ellipsoidal heat source model

### B. Finite Element Model

Based on ANSYS code, we developed a sequentially coupled thermo-elastic plastic finite element method to simulate the submerged arc welding process in a mild carbon steel plate. The flow chart of the sequentially coupled thermo-stress finite element analysis procedure is showed in Figure 2.

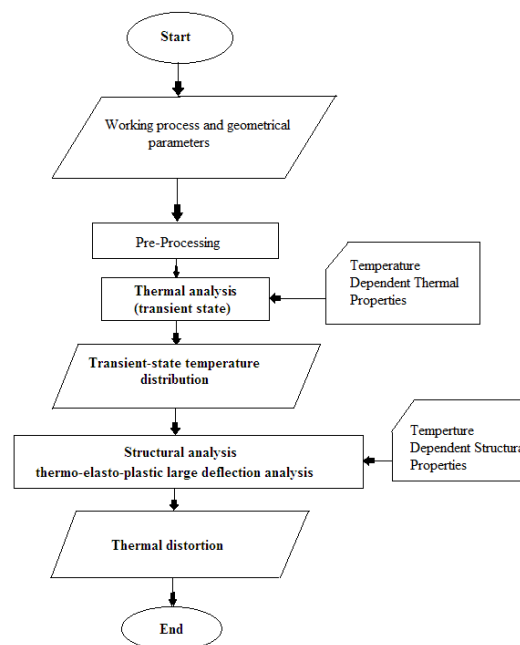


**Figure 2:** Flow chart of Thermal and Structural Finite Element Analysis Procedure [8].

### C. Element Type

In the present work, heat transfer analysis is conducted using element type SOLID70. This element type has a 3-D thermal conduction capability and eight nodes with a single degree of freedom (temperature) at each node. The element is applicable to a 3-D steady state or

transient thermal analysis. Since only one surface load can be applied on solid element SOLID70, shell element type SHELL57 was also used to simulate heat lost through convection and radiation on the surface. In structural analysis element type SOLID70 is replaced by a 3D structural element type SOLID45.

#### D. Material Properties

In the present work temperature dependent thermal and mechanical properties are employed for the effective modelling of the arc welding process. The material of the plate, used in the present work, is mild steel. Melting temperature of mild steel is 1505°C. Composition of mild steel in percentage of various alloying elements is given in Table 1.

**Table 1:** Composition of mild steel (in percentage)

C	Si	Mn	P	S	Ni	Cr	Fe
0.16	0.18	0.46	0.18	0.07	0.132	0.02	98.84

The thermal and temperature dependent mechanical properties of mild steel are given in Table 2 [6, 7].

**Table 2:** Thermal And Mechanical Properties of Steel

Temperature (°K)	Specific Heat (J/Kg-K)	Thermal Conductivity W/m-K	Poisson's ratio	Young's Modulus (GPa)	Thermal Expansion coefficient (10 <sup>-6</sup> m/°K)
0	450	51.9	0.278	200	10
373	499	51.1	0.309	200	11
573	565	46.1	0.331	200	12
723	630	41.05	0.338	150	13
823	705	37.5	0.357	110	14
873	773	35.6	0.373	88	14
993	1080.4	30.64	0.3738	20	14
1073	931	26	0.4238	20	15
1723	437.93	29.45	0.4738	2	-
1783	400	29.7	-	0.2	-
1853	735.25	29.7	-	0.00002	-
5273	400	42.2	0.499	0.00002	15.5

#### E. Boundary Condition

Thermal Boundary Conditions

##### I. First boundary condition.

A specified initial temperature covering the entire plate surface is

$$T = T_a \text{ for } t = 0$$

Where  $T_a$  is the ambient temperature. Energy balance at the work surface leads to the second and third boundary conditions.

In figure below Let un-meshed area represents A1, the zone where the arc heat is applied. The rest of the plate represented by A2, meshed area which is exposed to atmosphere where heat loss takes place due to convection in figure 3.

## II. Second Boundary Condition.

The arc heat acting over the surface A1, is given by

$$q_n = -q_{sup}$$

Or

$$-k \frac{\partial t}{\partial n} = -q_{sup} \text{ on the surface A1 for } t > 1$$

## III. Third Boundary Condition

The heat loss due to convection over A2 is given by

$$-k \frac{\partial t}{\partial n} = -h_f (T_a - T) \text{ on the surface A2 for } t > 0$$

Structural Boundary condition

Structural Boundary Conditions are shown in figure 4, where some constraints are applied on points and area in X.Y and Z directions.

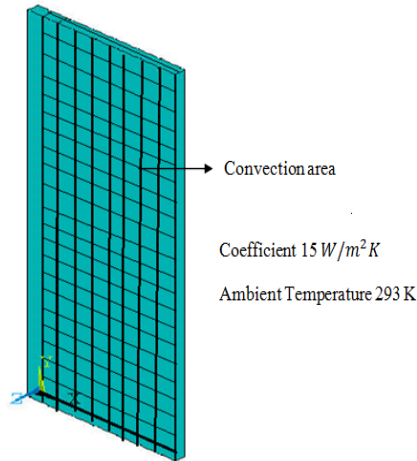


**Figure 3:** Thermal Boundary Condition

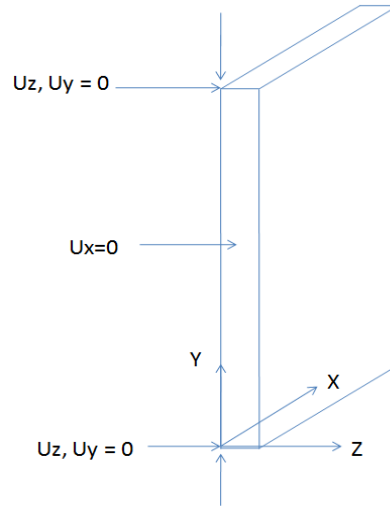


**Figure 4:** Structural Boundary Condition

## Result and Discussion

Highly non-uniform temperature applied during welding is a well-established cause of distortions in welded structures. The temperature profile and thus distortion depend largely on the welding parameters and geometrical parameters of the structure to be welded. Welding parameters such as welding current, welding speed and geometrical parameters have significant effect on distortions in welding. In this chapter results of FE model elaborated in previous chapters are discussed. Firstly the results on temperature profile and angular distortion are validated with the experimental or with the reported results in literature. Later a parametric study is performed.

The parameters are classified into two categories given as follow:

- Process parameters
  - Welding current
  - Welding speed
- Geometrical parameters
  - Plate thickness

Thermo-mechanical response, displacement is obtained from the finite element elasto-plastic analysis. For all cases, the responses at each node along the transverse direction are plotted over the nodes along the cross sections.

### A. Effect Of Welding Current

The relationship between the electrical energy and thermal heat is given by the following equation:

$$Q = \frac{V \times I \times 60}{v} \dots \quad (6)$$

Where,  $I$  is welding current;  $V$  is welding arc voltage;  $v$  is the arc welding speed, and  $Q$  is the heat input.

The effect of welding current on welding responses is evaluated using five values; 450, 500, 550, 600 and 650 Ampere. Rest other process and geometrical parameters are kept same.

The effect of varying welding current on the thermal response is illustrated in Figure 5. The results show that the welding current has a significant effect on the welding thermal response. When the heat input increases, the response peak temperature also increases. An increase of 50% in welding current results in a significant increase (1.5 times) in the peak temperature.

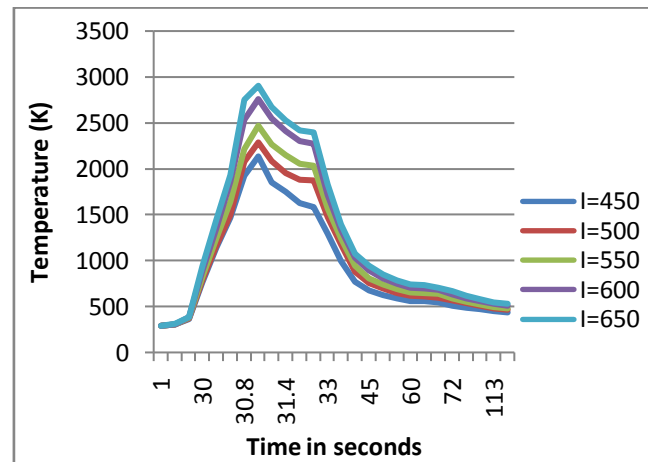


**Figure 5:** Temperature Distribution At Different Welding Current

The effects on the thermo-mechanical responses by varying welding current and keeping the other variables constant are illustrated in Table 4. The results show that the welding current has significant effect on the welding mechanical response. Increase in the welding current increases the mechanical displacement. An increase of 50% welding current results in a significant increase (1.3 times) in the Z displacement (Figure 6)

**Table 4:** Predicted Maximum Angular Distortion At Different Welding Current

Welding current (A)	Welding speed (mm/sec)	Plate Thickness (mm)	Predicted maximum angular distortion (mm)
450	5	10	0.870
500	5	10	0.961
550	5	10	1.037
600	5	10	1.124
650	5	10	1.170

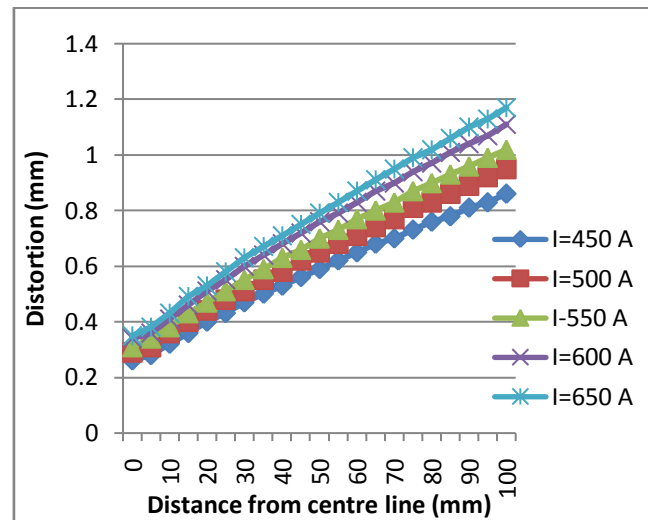


**Figure 6:** Comparison of Effect of Welding Current on Displacement

### B. Effects of Welding Speed

Welding speed represents the distance of the torch travelled along the weld line per unit of time. Heat input is inversely proportional to the welding speed (equation 6). Thus with lower values of the welding speed the magnitude of effective heat input increases for a constant heat input rate from source. In this work, different welding speeds are investigated while considering the rest of parameters constant. Different values of speed used in the finite element analyses are 4.50, 5.0, 5.5, 6.0 and 6.5 mm/sec.

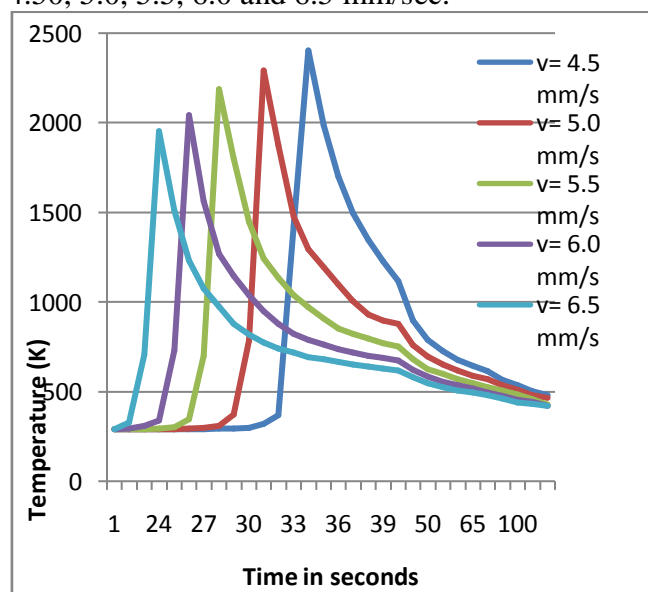


**Figure 7:** Temperature Distribution At Different Welding Speed

The effect of varying welding speed on the thermal responses is illustrated in Figure 7. The results show that the welding speed has a significant effect on the welding response. When the welding speed increases, the response peak temperature decreases and when the



welding speed decreases, the response peak temperature increases. A drop of 30 % of welding speed results in a significant increase in the peak temperature (1.25 times).

The effect on thermo-mechanical responses of varying welding speed keeping other process and geometrical parameters constant is illustrated in Table 5. As the welding speed increases, the displacement decreases. An increase of 1.4 times of the welding speed, for instance, results a decrease of 20% of z-displacement (Figure 8).

**Table 5:** Predicted Maximum Angular Distortion At Different Welding Speed

Welding current (A)	Welding speed (mm/sec)	Plate Thickness (mm)	Predicted maximum angular distortion (mm)
500	4.5	10	1.031
500	5.0	10	0.961
500	5.5	10	0.934
500	6.0	10	0.870
500	6.5	10	0.845

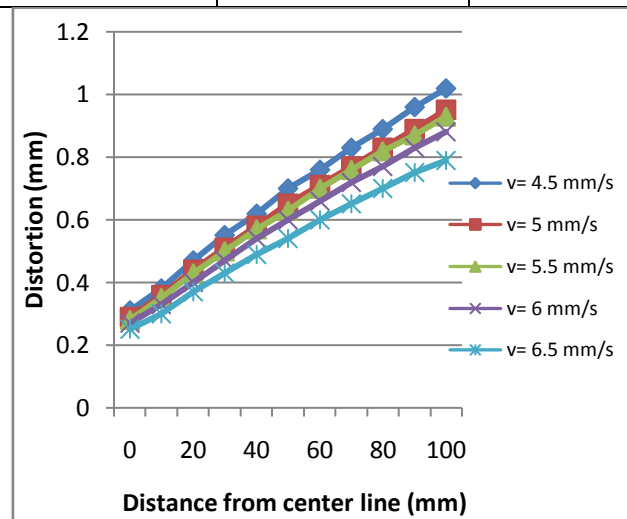


**Figure 8:** Comparison of Effect of Welding Speed on Displacement

### C. Effects of Plate thickness

Effect of variable plate thicknesses on temperature profile and maximum plate distortion is investigated. Other process parameters are kept constant at nominal range. Different values of plate thicknesses used for the finite element analyses are 7, 8, 9, 10 and 12 mm. The effects of varying plate thickness on the thermal responses are illustrated in Figure 9. The results show that the plate thickness has a significant effect on the welding response. For the thicker plate, the response peak temperature decreases, this is due to the higher rate of heat dissipation in case of the thicker plate. An increase of 1.7 times of plate thickness results in a significant decrease in the peak temperature (approximately 14%).

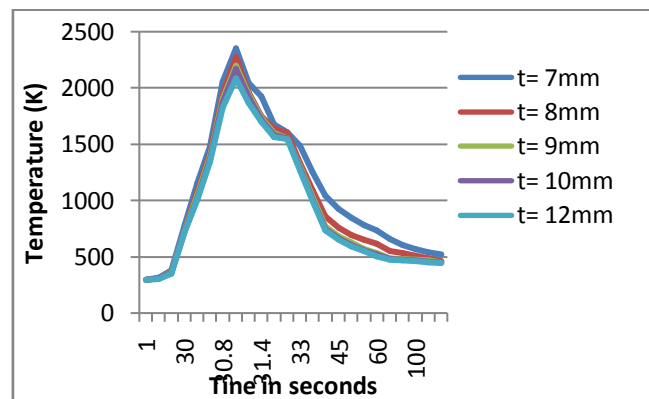


**Figure 9:** Temperature Distribution At Different Plate Thickness

The effects on the thermo-mechanical responses by varying plate thickness and keeping the other variables constant are illustrated in Table 6. The results show that the thickness has a significant effect on the welding mechanical response. When the thickness increases, the mechanical displacement response decreases. An increase of 1.7 times of plate thickness from 7 mm results in a decrease of approximately half of maximum angular distortion for plate thickness of 7 mm (Figure 10).

**Table 6:** Predicted Maximum Angular Distortion At Different Plate Thickness

Welding current (A)	Welding speed (mm/sec)	Plate Thickness (mm)	Predicted maximum angular distortion (mm)
500	5.0	7	1.741
500	5.0	8	1.219
500	5.0	9	1.084
500	5.0	10	0.961
500	5.0	12	0.718

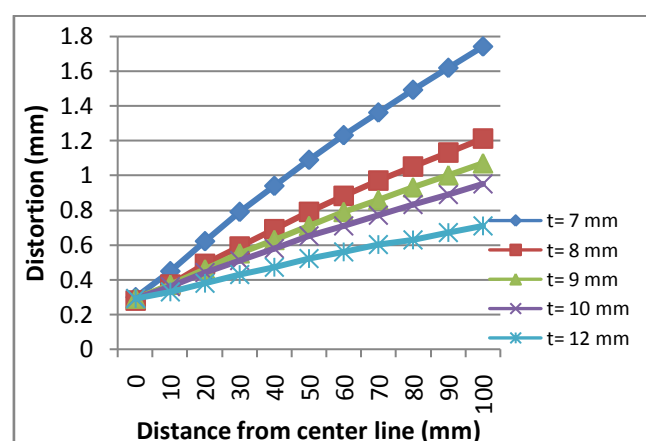


**Figure 9:** Comparison of Effect of Plate Thickness on Displacement

## **Conclusion**

The development of post-weld distortions in a welded structure is based intrinsically on the thermal cycle from the welding processes. Therefore, controlling the thermal cycle is critical to good quality welding. Computer-based simulative welding models that can predict process outcomes without the need for costly pre-production trials or experimentation will increasingly become essential tools for welding engineers. 3D nonlinear thermo-mechanical analyses using FEA method is performed to investigate the effects of welding parameters on transient temperature and distortions in simulation of butt joint submerged arc welding process.

Following are the outcome of the present FE study:

1. A complex welding process phenomenon can be simulated using a commercial finite element package, namely ANSYS®.
2. Double Ellipsoidal heat source model is more accurate than Gaussian heat flux distribution.
3. The distortion patterns obtained through finite element modelling are in good agreement with the experimentally observed patterns.
4. Based on the simulation results, distortion of the weldment can be predicted numerically. Thus, the experimental analysis, which might be costly, can be avoided.
5. Welding current, welding speed and thickness of plate have a significant impact on the thermal and mechanical responses.

The specific conclusion that can be drawn from the simulation results are as follows:

1. When the welding current increases, the response displacements also increases. An increase of 1.5 times of welding current results in a significant increase (1.3 times) in the z-displacement.
2. On the other hand, the opposite response behaviour is observed when the welding speed increases. An increase of 1.4 times of the welding speed, for instance, results a decrease of 20% of z-displacement.

The model with the lowest thickness set tends to have larger deformations. An increase of 1.7 times of plate thickness results in a significant decrease (approximately half of initial value) in the z-displacement.

## **References**

- [1] ZHU X.K., CHAO Y.J. , Effects of temperature-dependent material properties on welding simulation, *Computers and Structures* 80 (2002) 967–976 1973.
- [2] KIM, I.S., BASU A., A Mathematical Model of Heat Transfer and Fluid Flow in the Gas Metal Arc Welding Process, *Journal of Materials Processing Technology* 77 (1998) 17-24.
- [3] KOU, SINDO, *Welding Metallurgy*, Wiley, 2003
- [4] GOLDAK J.A., AKHLAGHI M., *Computational Welding Mechanics*, Springer 2005.
- [5] GOLDAK J., CHAKRAVARTI A., BIBBY M., A new finite element model for welding heat source , *Metall. Trans. B* (1984) 15B:299-305.
- [6] PATHAK A.K., DATTA G.L., Three-dimensional finite element analysis to predict the different zones of microstructure in SAW, *Proc. Instn Mech. Engrs Vol 218 Part B:J Engineering Manufacture*, (2004) 218:269-280.

- [7] AWANG H., The effects of process parameters on steel welding response in curved plates, Master of Science, College of Engineering and Mineral Resources, West Virginia, 2002.
- [8] GERY D., LONG H., MAROPOULOS P., Effects of welding speed, energy input and heat source distribution on temperature variations in butt joint welding, J. Materials Processing Tech. (2005) 167:393-401.
- [9] HUSSAIN I.A., Study of thermal distortion in thick plate using finite element technique, J. Engineering and Development (2008) 12:118-130.